



Catalytic steam reforming of the aqueous fraction of bio-oil using Ni-Ce/Mg-Al catalysts

F. Bimbera ^{a,b,1}, J. Ábreo ^{a,b}, R. Puerta ^b, L. García ^{a,b,*}, J. Arauzo ^{a,b}

^a Grupo de Procesos Termoquímicos (GPT), Aragón Institute for Engineering Research (I3A), Universidad de Zaragoza, Mariano Esquillor s/n, 50018 Zaragoza, Spain

^b Chemical and Environmental Engineering Department, Universidad de Zaragoza, María de Luna 3, 50018 Zaragoza, Spain

ARTICLE INFO

Article history:

Received 4 October 2016

Received in revised form 27 February 2017

Accepted 1 March 2017

Available online 4 March 2017

Keywords:

Bio-oil

Steam reforming

Nickel

Cerium

Hydrogen

ABSTRACT

The performance of different Ni/Mg-Al catalysts modified with Ce was evaluated in the catalytic steam reforming of aqueous fractions of bio-oil from biomass pyrolysis. The effects of several preparation methods for incorporating Ce as a modifier (co-precipitation, impregnation and direct thermal decomposition of the salt precursors), the Ce content (0–5 wt.%) and the feed streams (three different aqueous fractions from bio-oil) on the catalyst performance were examined, and it was found that the stability and activity of the catalysts were significantly influenced by all these factors. In general, the addition of Ce to a reference Ni/Mg-Al catalyst improved the overall carbon conversion to gas and the yield to H₂ as well as enhancing the catalyst stability in the steam reforming of aqueous fractions of bio-oils. The best preparation method was impregnation and the optimal Ce content was found to be 0.5 wt.%. Much higher initial carbon conversion to gas and initial H₂ yields was obtained using bio-oils derived from pine than those derived from poplar. A very low coke formation, 103 mg C/(g of catalyst · g of organics in the aqueous fraction reacted), was achieved using the optimized catalyst, 0.5 wt.% Ce prepared by impregnation.

© 2017 Elsevier B.V. All rights reserved.

1. Introduction

Biomass pyrolysis liquids differ significantly from petroleum-based fuels both in physical properties and in chemical composition. The high oxygen content results in a low energy density (heating value), which is less than 50% of that for conventional fuel oils. Light fuel oil consists mainly of saturated and aromatic hydrocarbons (C₉–C₂₅) while pyrolysis liquids contain a large amount of compounds with oxygen (alcohols, ketones, acids, etc.) [1,2].

The main applications of bio-oil or its fractions have been described in the literature [3–5]. Basically, bio-oils can be used as fuels and/or for the production of chemicals. The fuel applications of bio-oils mainly comprise combustion in burners, furnaces, boilers, Diesel and Stirling engines and turbines. There are, however, some drawbacks in their combustion [4].

Bio-oil constitutes an attractive feedstock for the production of valuable chemicals because of its high abundance in carbonyl, carboxyl and phenolic groups. Some authors have studied the thermochemical conversion of crude bio-oil into various products through several processes such as hydrotreating [6], upgrading over zeolites [7], catalytic cracking [8,9] or steam gasification [10].

Another interesting possibility is the catalytic steam reforming of liquid pyrolysis products or their fractions, aiming at the production of a hydrogen-rich product gas [11]. A separation of the bio-oil into two phases can be done by water addition. These phases are a lignin-derived fraction, which would be devoted to the production of fine chemicals due to its high content in phenolic compounds, and a carbohydrate-rich aqueous fraction that would be subjected to catalytic steam reforming for the production of hydrogen [12,13].

The NREL proved that sustainable H₂ production by catalytic steam reforming of the aqueous fraction of bio-oil can be economically viable if a process based on the coproduction of H₂ and fine chemicals can be developed [4,12,14].

Many studies have used bio-oil model compounds to study the catalytic steam reforming process, as described in some review papers [15,16]. In previous works conducted by our research group, acetic acid [17–19], acetol [20–22], and butanol [21] were selected as model compounds representing the major functional groups present in the aqueous fraction of bio-oil. Nonetheless, some

* Corresponding author at: Grupo de Procesos Termoquímicos (GPT), Aragón Institute for Engineering Research (I3A), Universidad de Zaragoza, Mariano Esquillor s/n, 50018 Zaragoza, Spain.

E-mail address: luciag@unizar.es (L. García).

¹ Present address: Grupo de Reactores Químicos y Biorreactores, Applied Chemistry Department, Universidad Pública de Navarra, 31006 Pamplona, Spain.

authors have previously steam reformed the actual bio-oil or its fractions [11–13,23–32].

The development of suitable catalysts for the process has been the subject of numerous studies. These can be divided into two main categories: supported noble metal catalysts and Ni-based catalysts, both commercial and laboratory prepared. The main advantage of Ni-based catalysts compared to those based on noble metals is their high activity and selectivity towards H₂ production at a much cheaper cost [11,12,17–23,25,30,33]. However, Ni-based catalysts are more susceptible to carbon formation [23]. Hence, the development of Ni-based catalysts more resistant to deactivation by coke deposition remains a challenge.

The strategies to enhance the resistance to deactivation by carbon deposits in steam reforming Ni-based catalysts can be basically divided into two: the enhancement of water adsorption on the catalyst support in order to gasify coke or coke precursors, and the modification of active metal surfaces via the presence of other metals [23,34,35]. The use of Mg as a modifier of Ni/Al catalysts prepared by coprecipitation has revealed enhanced resistance to deactivation by coke deposition in the catalytic steam reforming of biomass oxygenates [36] and aqueous fractions of bio-oil [32,37].

One of the approaches that poses a promising alternative is the use of rare earths such as lanthanides. Lanthanides have been reported to enhance catalytic activity and stability as textural promoters of Ni-based catalysts, since they inhibit both the growth of nickel crystallites and the carbon deposition on catalyst surfaces [23,38]. In particular, the addition of La as a textural promoter on Ni-Al catalysts has been reported to be beneficial as a result of an enhanced resistance to carbon deposition on the catalyst surface [8,18,20,23,39–41].

Another possibility that has been addressed by some researchers is the use of cerium oxides as promoters of Ni-based catalysts because of their good properties for oxidizing dehydrogenated carbon species deposited on the catalyst surface in the steam reforming of oxygenates such as acetic acid [42], ethanol [42,43] and *n*-butanol [44]. Some authors have tested Ni/Al catalysts modified with Ce in the catalytic steam reforming of the aqueous fraction of bio-oils from corn stalk [37,45] and from oil-seed camellia [46]. Yao et al. [37] incorporated a relatively high atomic content of Ce in the mixed Al-Ce oxides. Fu et al. [45] and Xu et al. [46] opted for a different approach using low amounts of Ce as a promoter in the different Ni-Ce/Al formulations, which were obtained by co-impregnation of commercial γ-Al₂O₃ supports. The oxidation of the surface carbon species deposited on the surface was enhanced by the incorporation of Ce and facilitated their gasification in the form of carbon oxides [47], thus increasing the resistance of the catalyst against deactivation by the deposition of carbonaceous deposits on the catalyst.

The objective of the present work is to evaluate the catalyst performance of Ni/Mg-Al modified with Ce in the reforming of the aqueous fraction of bio-oil. The effects of the catalyst preparation method, the cerium content, and the characteristics of the bio-oils used as feed (raw material and fast pyrolysis technology) on the catalyst performance have been examined.

The catalyst performance has been compared in terms of the yield to hydrogen, the degree of conversion of the aqueous fraction, the catalyst activity and the catalyst deactivation.

2. Experimental

2.1. Experimental system

The experimental installation used is a microactivity unit designed and built by PID (Process Integral Development Eng & Tech, Spain). The unit consists of a small bench scale rig comprising

a fixed bed placed inside a tubular reactor (made of quartz in order to avoid any catalytic wall effects), a high-performance liquid chromatography (HPLC) pump to feed the aqueous fraction of bio-oil at a specified rate, a condenser to separate condensates from permanent gases at the outlet of the reactor, and a gas chromatograph (Micro-GC Agilent G2801A) to analyse these gases. The feed inlet of the reactor was designed to avoid polymerization of the oligomers and sugars present in the aqueous fraction of bio-oil, which may cause clogging of the inlet. The aqueous fraction of bio-oil was fed into the reactor in a spray form with the aid of a N₂ stream. A general description of the installation and the feeding system can be found in previous works [17,31].

The experimental system operated at atmospheric pressure with a total N₂ flow rate of 80 cm³(STP)/min. The catalytic bed was formed by 0.07 g of catalyst mixed with silica sand (1.80 g approx.) with a particle size ranging between 165 and 315 μm. Steam reforming experiments were conducted for 2 h with a reaction temperature of 650 °C, an aqueous fraction flow rate of 0.12 mL/min and a constant space velocity (G_{C1}HSV) of 13,000 h⁻¹. G_{C1}HSV is defined as the volume of C1-equivalent species in the feed at standard temperature and pressure (STP) per unit volume of catalyst bed (including the void fraction) per hour [33].

2.2. Aqueous fraction of bio-oil

Three different aqueous fractions were used, coming from two different bio-oil production technologies and suppliers: a rotating cone reactor owned by the Dutch company Biomass Technology Group BV (BTG) and a spouted bed reactor owned by the Ikerlan Research Centre located in the Basque Country, Spain.

The aqueous fractions of the different bio-oils were prepared following the procedure described in a previous work [31].

The characterization of the different aqueous fractions prepared from bio-oils is presented in Table 1. The elemental compositions of the aqueous fractions and empirical formulas for the organics present in the mixture are similar to others found in the literature [25,26,31,48].

2.3. Catalyst preparation

Different Ni-Ce/Mg-Al catalysts with the same Ce content (3% mass fraction) were prepared in the laboratory using various techniques, including coprecipitation at increasing pH, coprecipitation at constant pH, incipient wetness impregnation and thermal decomposition of the precursor salts. These catalysts were used for studying the influence of the preparation method. A reference Ni/Mg-Al catalyst having a Ni relative atomic content of 28% expressed as Ni/(Ni + Al + Mg) was prepared by coprecipitation at increasing pH following the same procedure as that described in our previous works [17,21,31,32].

The catalyst prepared by coprecipitation at constant pH was prepared following a variation of a method developed by Bhattacharyya et al. [49,50] which is detailed elsewhere [36]. The novelty in this work is the addition of Ce(NO₃)₃·6H₂O (Sigma-Aldrich, 99.999% purity) to the solution of nitrate precursors of the different metals. The amounts of the different nitrate precursors added to the solution were calculated so as to have a calcined precursor with a final content of 3% Ce and to maintain the same molar ratios as the reference catalyst [32]: Ni/Al = 0.49, Mg/Al = 0.26 and 28% relative atomic percentage, Ni expressed as Ni/(Ni + Al + Mg + Ce). Hence, the amounts of different metal nitrates added to the solution were as follows: 6.69 g of Ce(NO₃)₃·6H₂O, 47.17 g of Mg(NO₃)₂·6H₂O (Fluka, puriss. p.a. ACS 99% purity), 265.43 g of Al(NO₃)₃·9H₂O (Merck, 95% purity), and 100.80 g of Ni(NO₃)₂·6H₂O (Merck, 99% purity).

Table 1
Characteristics of the aqueous fractions.

H ₂ O content (% mass fraction)	BTG pine, rotating cone (RC-Pi) 84.23	IKERLAN pine, spouted bed (SB-Pi) 83.99	IKERLAN poplar, spouted bed (SB-Pp) 83.03
Ultimate analysis (% mass fraction)			
C	7.35	7.36	7.28
H	10.82	10.61	10.95
N	0.00	0.59	0.12
O ^a	81.83	81.43	81.65
Empirical formula (organics) ^b			
CH _x O _y	CH _{2.39} O _{0.71}	CH _{2.08} O _{0.69}	CH _{2.85} O _{0.81}
Molecular mass (organics) g/mol	25.75	25.12	27.78
H ₂ O/C molar ratio	7.64	7.61	7.60
Density g/mL	1.03	1.05	1.03

^a determined by difference.

^b Nitrogen not taken into consideration in the empirical formula.

The hydrated precursors of all these catalysts were calcined under air flow at a temperature of 750 °C. This final calcination temperature was maintained for three hours.

In addition, several Ni-Ce/Mg-Al catalysts with varying Ce content (0–5% mass fraction) were prepared under the incipient wetness impregnation technique. The preparation of the calcined precursor was done by adding the required amount of Ce to the calcined precursor of the reference catalyst to obtain the desired Ce content in the final precursor. After the dropwise addition of the solutions containing the Ce nitrates to the calcined Ni/Mg-Al-O solid serving as support, the samples were further dried at 105 °C overnight and subsequently calcined following the conditions detailed above in order to obtain the definitive calcined precursors of the Ce-containing catalysts prepared by impregnation.

Finally, a Ni-Ce/Mg-Al catalyst was prepared by direct thermal decomposition of the metal nitrates. The metal nitrates decompose into their corresponding oxides following several steps as the temperature increases [51,52]. The main advantage of such a preparation technique lies in its simplicity, achieving the calcined precursor in a single direct step from the metal precursors.

The preparation of the calcined precursor was carried out as follows. The same amounts of the metal nitrates as those detailed for the preparation of the constant pH precursor were ground together in a mortar to obtain an intimate mixture of the chemicals. This was calcined in a porcelain crucible in the muffle furnace using the following calcination program. Initially, a heating ramp of 6 °C/min was selected in order to increase the temperature up to 120 °C. Then, a ramp of 3 °C/min was used until 200 °C was reached. In order to have a controlled release of the NO_x gases, a ramp of 1 °C/min was selected until a temperature of 320 °C was achieved. Afterwards, the heating rate was increased again (4 °C/min) up to 700 °C and a final ramp of 1.5 °C/min led to the final calcination temperature of 750 °C, which was maintained for 3 h. Finally, the calcined precursor was cooled down to room temperature.

All the calcined precursors were sieved in order to obtain a particle size distribution between 160 and 315 micrometres.

Prior to the reaction, all the calcined precursors were reduced in situ for 1 h at 650 °C using diluted hydrogen (10 vol.%) in a nitrogen-rich stream.

2.4. Catalyst characterization

The calcined precursors of the different catalysts were characterized using different techniques, including elemental analysis by

optical emission spectrometry combined with inductively coupled plasma (ICP-OES), X-ray diffraction (XRD), N₂ adsorption and temperature programmed reduction (TPR). The ICP-OES, XRD and TPR measurements were done following procedures that are detailed elsewhere [36].

The calcined precursors of the catalysts were analyzed by nitrogen adsorption in a Micromeritics TriStar II 3000 V6.08A analyzer. The adsorption and desorption isotherms were obtained using static volumetric measurements at 77 K and room temperature, respectively, with previous preconditioning of the samples (degas) at 200 °C during 8 h in inert gas flow (N₂). The surface area of the different samples was determined using the Brunauer-Emmett-Teller (BET) method. The pore size distribution was calculated using the Barrett-Joiner-Halenda (BJH) method, by means of the differential pore volume calculated by deriving the cumulative pore volume with respect to the pore diameter, considering a diameter range from 1.7 to 300 nm.

Spent catalysts were characterized by elemental analysis, transmission electron microscopy (TEM) and XRD. A LECO Truspec Micro model was the equipment used for carrying out the elemental analysis. TEM images were obtained with a JEOL-2000 FXII microscope. The XRD diffractometer was the same as that used in the characterization of calcined precursors. In addition, some spent catalyst samples were characterized by temperature-programmed oxidation (TPO) after being used in some experimental runs. Details about the procedure and equipment used in the TPO technique are described in a previous work [36].

2.5. Thermodynamic calculations

The equilibrium values of the different product gases were calculated with the Aspentech HYSYS 3.2 simulation software by means of minimization of the Gibbs free energies. To do so, a Gibbs reactor module was selected with a PRSV thermodynamic package. The bio-oil aqueous fractions were simulated by taking into account the data from their ultimate analyses. Further details can be found elsewhere [31].

3. Results and discussion

3.1. Characterization of the calcined precursors

3.1.1. Elemental analysis by ICP-OES

Table 2 shows the elemental analyses of the catalysts containing 3% of Ce and prepared by the different coprecipitation, thermal

Table 2

Theoretical and experimental (elemental analysis by ICP-OES) composition of the catalysts.

Catalyst Preparation Method	% mass fraction							
	Ce		Mg		Al		Ni	
Theor.	Experim.	Theor.	Experim.	Theor.	Experim.	Theor.	Experim.	
Coprecipitation, increasing pH	3.00	2.74	6.20	7.49	26.50	28.05	28.25	24.54
Coprecipitation, constant pH	3.00	2.77	6.20	7.10	26.50	26.57	28.25	27.21
Thermal decomposition	3.00	1.54	6.20	6.71	26.50	25.86	28.25	29.94
Impregnation, 0.5% Ce	0.50	0.48	6.20	6.59	26.50	27.19	28.25	29.16
Impregnation, 1% Ce	1.00	1.01	6.20	6.49	26.50	26.65	28.25	29.58
Impregnation, 3% Ce	3.00	3.23	6.20	7.01	26.50	27.26	28.25	25.86
Impregnation, 5% Ce	5.00	5.19	6.20	6.25	26.50	25.83	28.25	27.06

decomposition and impregnation techniques, as well as those catalysts prepared with different Ce contents. Comparisons with the theoretical compositions are also provided.

As can be seen, the Ce content is very close to the expected theoretical value in all cases, which means that this element was successfully incorporated into the catalyst structures (with the sole exception of the catalyst prepared by thermal decomposition). In contrast, Ni contents are somewhat lower than expected in certain samples (coprecipitated, 3 and 5% catalysts prepared by impregnation). This could be attributed to an incomplete incorporation of Ni during the preparation of the hydrated precursors, due to the formation of complexes, especially between Ni and ammonia [53]. Interestingly, the catalysts prepared by direct decomposition of the nitrate precursors and 0.5 and 1% Ce prepared by impregnation show greater Ni contents than the theoretical values.

3.1.2. X-ray diffraction

The calcined precursors containing Ce and prepared under the different techniques previously described were analysed by XRD. Fig. 1a shows the diffraction patterns of the different samples containing 3% Ce and that of the Ni/Al-Mg reference catalyst. The catalysts prepared with different Ce contents by impregnation presented similar diffraction patterns and are depicted in Fig. 1b, for the sake of clarity. All the samples were compared to standard diffraction patterns using the library package from the analyser software containing diffraction patterns from the JSBD database.

The calcined samples of the catalyst prepared by thermal decomposition of the nitrate precursors and by coprecipitation at constant pH present the most crystalline structures.

The crystalline phase corresponding to CeO_2 could be identified in both samples. This phase could also be detected in the calcined samples of the catalysts prepared by impregnation.

Similarities between the main peaks found in the different samples and in the reference material Ni/Mg-Al can be explained by the existence of several Ni- and Mg-containing oxides and spinels. The overlapping of peaks makes the precise identification of each species difficult; however, the main peaks found at 37 and 43° could be attributed to a solid solution $\text{NiO}\cdot\text{MgO}$, because both compounds crystallize into the same structure [54].

Fig. 1b clearly shows the increase of the CeO_2 crystalline phase as the Ce content increases.

3.1.3. Temperature programmed reduction (TPR)

The normalized TPR profiles of the different calcined precursors from the catalysts containing 3% Ce are presented in Fig. 2a. For the sake of comparison, the TPR profile of the reference catalyst has also been included. All the precursors present a maximum reduction peak, the Ce-containing catalyst prepared at constant pH being the only one not showing shoulders or peaks overlapping its maximum peak. In this catalyst, two other peaks are observed at 468 and 971 °C respectively. The presence of these two peaks could be attributed to the reduction of the $\text{Ce}^{4+}/\text{Ce}^{3+}$ redox pair, which

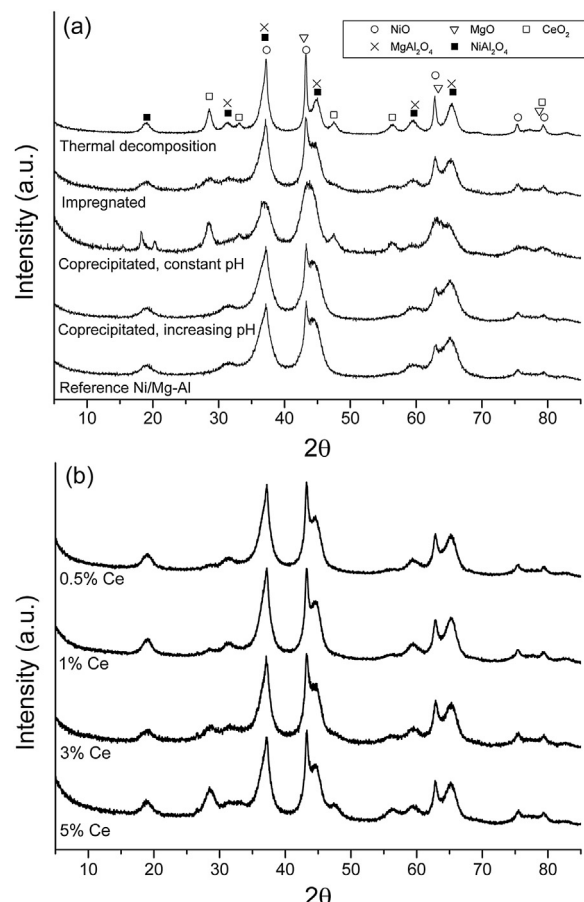


Fig. 1. XRD patterns of the calcined precursors a) reference and with 3% Ce prepared by different methods, (b) with varying Ce content by impregnation.

takes place in two steps. Thus, the peak found at 468 °C could correspond to the first step, where there is a reduction of the oxygen contained in the surface CeO_2 species, showing a weak interaction with the catalyst support. The peak at 971 °C could correspond to the reduction of the oxygen from the CeO_2 species integrated within the crystalline network, hence presenting a strong interaction with the different spinel phases from the support, in agreement with previous findings described in the literature [55].

Other calcined precursors, such as those prepared by the increasing pH and the thermal decomposition techniques, show a smooth slope rising before reaching the maximum reduction peak, which is broad and starts at reduction temperatures of around 400 °C. This section of the profiles can be attributed to the reduction of NiO species having a weak interaction with the support [56].

Regardless of the preparation technique, it can be observed that the temperature values corresponding to the maxima of the main

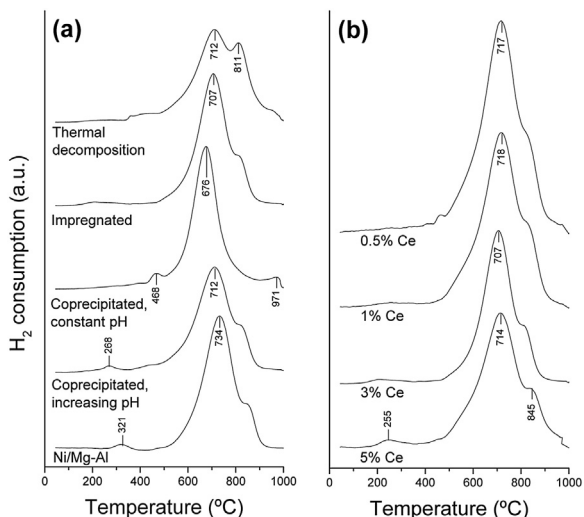


Fig. 2. (a) TPR profiles of the calcined precursors with 3% Ce, (b) catalysts prepared with varying Ce content by impregnation.

reduction peaks of the different samples decrease when cerium is incorporated in the catalyst. The maximum reduction peak has been attributed to the reduction of the spinel $NiAl_2O_4$ species [22]. The lowest temperature value of the different maxima from the main reduction peaks corresponds to the Ce-containing catalyst prepared by the coprecipitation method at constant pH, $676^{\circ}C$.

The shoulders observed for the catalysts prepared by coprecipitation at increasing pH and impregnation, as well as the maximum at $811^{\circ}C$ found for the catalyst prepared by thermal decomposition, are attributed either to the existence of different NiO - MgO species that show a greater interaction, as a result of being part of a solid solution, or to the presence of $MgAl_2O_4$ spinels [36]. Finally, the catalysts prepared with varying Ce content by impregnation had a very similar TPR profile, shown in Fig. 2b for the sake of clarity. It could be observed that the maxima of the main reduction peaks are very similar (between 707 and $718^{\circ}C$ in all cases) and that there is a more pronounced shoulder with increasing Ce contents. Interestingly, Ce contents below 5% Ce had a maximum at around $825^{\circ}C$, but the 5% Ce catalyst presented this maximum at around $845^{\circ}C$. This could be attributed to a more significant presence of CeO_2 species integrated within the crystalline network, which would result in a more accentuated reduction of these species with increasing Ce loading, in agreement with the previous discussion (see above). The catalyst prepared by impregnation with 5% Ce shows a small peak at low temperatures, around $250^{\circ}C$, which can be attributed to the existence of NiO species having low interaction with the support.

3.1.4. Nitrogen adsorption measurements

Table 3 shows the results of the N_2 adsorption measurements. The surface areas of the different samples in this work are in the range of similar Ni/Mg-Al catalysts containing Ce as a promoter, either prepared by impregnation [43] or by coprecipitation at constant pH [57]. The addition of Ce as a promoter results in a significantly decreased surface area, compared to that of the reference sample. In particular, if the reference catalyst and the sample prepared by coprecipitation at constant pH are compared, it can be observed that the surface area is decreased by around a quarter by the addition of Ce to the precursor. This could be explained by the fact that CeO_2 solids have low surface areas as a result of being non-porous materials [55].

The results shown in Table 3 also reveal that the preparation technique has an influence on the resulting surface area of the Ce-containing catalysts, even if the theoretical amounts of the metal

precursors added in the catalyst preparation and the calcination conditions are the same. The lowest values were obtained for the catalyst prepared by thermal decomposition, which had a surface area around a third of that obtained for the reference catalyst and less than half of that obtained for any of the catalysts prepared with a 3% of Ce load using different techniques. Its pore volume was also the lowest, a half or even less than that of the rest of the catalysts.

Interestingly the catalyst prepared at constant pH has the greatest pore volume and average pore diameter, even greater than those of the reference catalyst. These results are consistent with other previous results of a Ni/Mg-Al catalyst prepared by coprecipitation at constant pH [36]. The nature of the compensating anion could explain these results. The type of compensating anion, the average pore diameter and the pore volume are modified, particularly if vaporizable anions are present [58]. When nitrates are the compensating anion, the surface area of the resulting calcined solids is typically lower by a factor of two compared to that of precursors prepared with carbonates as compensating ions [59]. Lastly, the development of the porosity of solids prepared by calcination of double layered hydroxides is greater than in those materials prepared by direct thermal decomposition of the metal nitrates as a result of possible sintering phenomena during the calcination of the latter, which could yield larger crystal sizes and show a higher degree of crystallinity at the expense of a lower development of porosity. This is in agreement with the XRD analyses previously shown and with the observations made in other studies [60].

3.2. Catalytic steam reforming of aqueous fraction of bio-oil

The catalytic reforming experiments study the influence of (a) the catalyst preparation method, (b) the Ce content of the catalysts, (c) the aqueous fraction composition.

3.2.1. Effect of the catalyst preparation method

The performance of the catalysts containing 3% (m/m) Ce and the Ni/Al-Mg reference material were compared by carrying out experiments at the same catalyst load, temperature and $G_{C_1}HSV$, as described in the Experimental Section. In all these experiments, the aqueous fraction fed into the reactor was the one prepared from BTG's bio-oil.

The overall results of the gas, liquid and solid yields, as well as the gas composition (on a dry and nitrogen-free basis), are shown in Table 4. The mass balance closure for these experiments ranged between 91 and 94%.

Carbon conversion to gas (defined as the percentage of C in gases of a total organic C fed) was also calculated. The average carbon conversion to product gases was over 65% using the Ce-containing catalysts, with the exception of the coprecipitated catalyst at increasing pH. With the exception of the latter, the incorporation of Ce as a promoter resulted in an enhancement of the carbon conversion to gas compared to that of the reference catalyst, particularly in the case of the impregnated catalyst which yielded the greatest value of carbon converted to gas.

Fig. 3 shows the evolution of the H_2 yield (defined as g of H_2 produced per g of organic compounds in the feed) throughout the experiments. The time evolution of the yield to CO_2 presents similar trends and thus it has not been depicted, whereas the evolution of the CO yield over time (also not depicted) does not show clear trends, with the different yields obtained with the catalyst tested showing values close to the thermodynamic equilibrium value. It can be seen in Fig. 3 that the catalyst prepared by coprecipitation at increasing pH shows a distinct behaviour, producing significantly lower hydrogen yields. The catalyst prepared by coprecipitation at constant pH shows a H_2 yield that is similar to that obtained using the reference catalyst. The catalyst prepared by thermal decomposition shows a higher H_2 yield than the reference catalyst at low

Table 3
Nitrogen adsorption analyses.

Catalyst	Surface area (BET) (m^2/g)	Pore volume (cm^3/g)	Average pore diameter (nm)
Reference Ni/Mg-Al	161	0.21	4.8
Impregnated 3% Ce	129	0.23	5.3
Coprecipitated increasing pH 3% Ce	139	0.27	6.2
Coprecipitated constant pH 3% Ce	124	0.40	9.5
Thermal decomposition 3% Ce	55	0.09	5.5
Impregnated 0.5% Ce	145	0.21	5.6
Impregnated 1% Ce	125	0.21	6.5
Impregnated 5% Ce	134	0.18	5.2

Table 4
Overall product yields and gas composition. Experiments using catalysts with 3% Ce. Reaction temperature = 650 °C and $G_{\text{C}_1\text{HSV}} = 13,000 \text{ h}^{-1}$.

Catalyst	Reference, Ni/Mg-Al	Coprecipitated at increasing pH	Coprecipitated at constant pH	Impregnated	Thermal decomposition
Gas Yield (g/g liquid fed)	0.174	0.124	0.179	0.193	0.178
Liquid Yield (g/g liquid fed)	0.765	0.791	0.737	0.714	0.728
Solid Yield (g/g liquid fed)	0.015	0.015	0.015	0.014	0.016
Average carbon conversion to gas (%)	66.1	53.9	68.9	72.5	67.3
Gas composition (vol.%)					
H ₂	68.6	64.1	67.2	68.8	68.8
CO	8.2	14.7	7.5	7.6	7.8
CO ₂	22.1	17.3	23.1	22.7	22.3
CH ₄	0.9	3.2	1.8	0.6	0.8

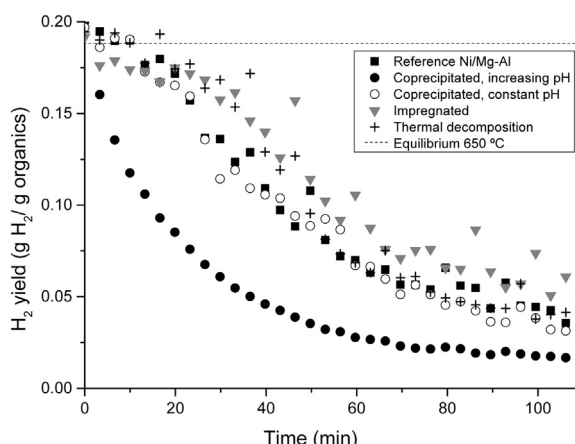


Fig. 3. Evolution of H₂ yield. Experiments with catalysts containing 3% Ce. Reaction temperature = 650 °C and $G_{\text{C}_1\text{HSV}} = 13,000 \text{ h}^{-1}$.

reaction time, less than 50 min. The catalyst prepared by impregnation shows a higher H₂ yield than the reference catalyst from 20 min to the end of the test. For instance, the one prepared by impregnation produced an average H₂ yield of 0.123 g H₂/g organics in the feed, while the reference material produced 0.111 g H₂/g organics in the feed.

Nonetheless, it is noticeable that the initial hydrogen yields for the different catalysts tested are at equilibrium conditions under the experimental conditions tested. It is clear that the catalyst prepared by impregnation shows the best H₂ yield. The use of less severe operating conditions, temperatures higher than 650 °C and space velocities smaller than 13,000 h⁻¹, could show the significant improvement of incorporating cerium in the catalyst prepared by impregnation compared to the reference catalyst. The evolution of carbon conversion to gas with time reveals a decreasing trend in most of the tested catalysts, likely caused by coke deposition on their surface [31]. This is in accordance with the observed gradual increase of light hydrocarbons (CH₄ and C₂s) in the product gas, as can be seen in Fig. 4. The decrease of carbon conversion to gas over time as a result of deactivation by the formation of coke

implies that progressively lesser amounts of CO and CO₂ are formed over time, since the steam reforming reaction to produce CO is significantly affected by the catalyst deactivation. Subsequently, the decrease in hydrogen yield over time can thus be explained as a result of decreased catalytic activity in the reforming reaction in combination with the modified equilibrium of the WGS reaction.

From these results, it can be concluded that the catalyst preparation method influences the catalyst stability in the catalytic steam reforming of the bio-oil aqueous fraction under given experimental conditions.

Table 5 shows the carbon content in the spent catalysts determined by elemental analysis. The results indicate a significant decrease in carbon content for the catalyst prepared by impregnation. Although the overall cerium content is the same for all the catalysts (except the reference one, which does not contain Ce), the interaction with superficial nickel should be greater in the case of the impregnated catalyst owing to the fact that most of the cerium must be on the surface of the catalyst as a result of the preparation procedure followed. The oxidative ability of cerium explains the decrease in carbon content in the impregnated catalyst. The coprecipitated catalyst prepared at increasing pH has a slightly lower amount of carbon than the reference catalyst; a more significant decrease is observed for the catalyst prepared by coprecipitation at constant pH, while the catalyst prepared by thermal decomposition has a greater amount of carbon than the reference catalyst. These results indicate that the carbon content in the used catalysts is not the only reason for the decrease in hydrogen yield with time. Thus, the catalyst prepared by coprecipitation at increasing pH shows the greatest decrease in hydrogen yield although it does not have the highest carbon content on the spent sample. In contrast,

Table 5
Carbon content in spent catalysts with 3% Ce and the reference catalyst.

Catalyst	Carbon (%)
Reference	20.99
Coprecipitated increasing pH 3% Ce	19.32
Coprecipitated constant pH 3% Ce	16.24
Impregnated 3% Ce	10.56
Thermal decomposition 3% Ce	23.87

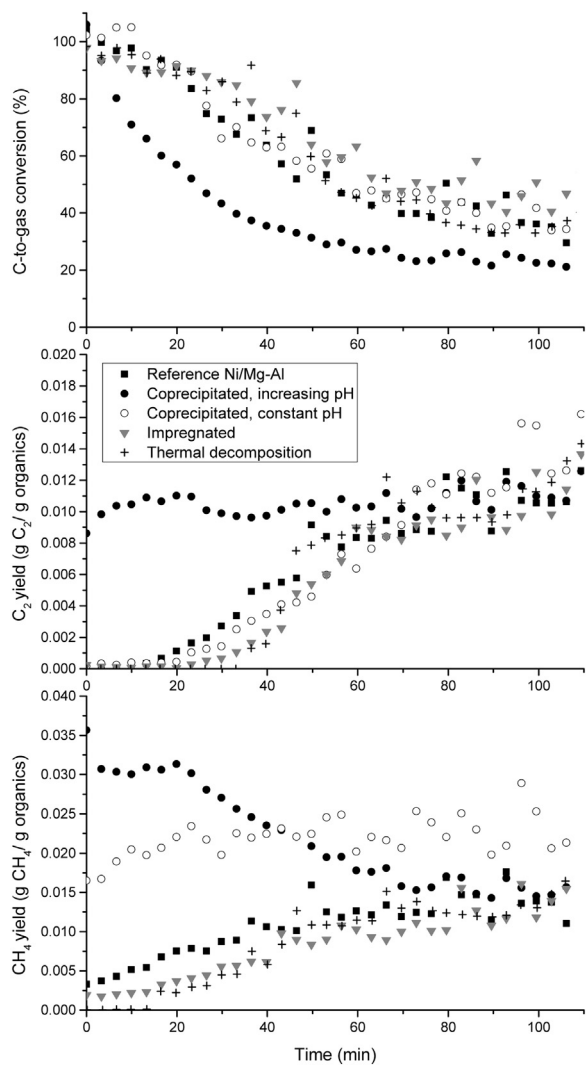


Fig. 4. Evolution of carbon conversion to gas, C_2 , and CH_4 yields. Experiments with catalysts containing 3% Ce. Reaction temperature = $650^\circ C$ and $G_{C1HSV} = 13,000\text{ h}^{-1}$.

impregnated catalyst and the catalyst prepared by coprecipitation at constant pH show a low decrease in H_2 yield with time but these catalysts have low carbon contents in their corresponding spent samples.

Fig. 5 shows representative TEM images of the spent catalysts. All the images show the presence of carbon filaments.

The reference catalyst shows carbon filaments with a wide range of diameter sizes, from 25 to 100 nm. Nickel particles have been detected for this catalyst with sizes from 50 to 150 nm. The coprecipitated catalyst prepared at increasing pH shows carbon filaments with diameters ranging from 17 to 270 nm, and the nickel particles detected have sizes from 22 to 150 nm. The coprecipitated catalyst prepared at constant pH shows carbon filaments with diameters between 16 and 125 nm, while the majority of nickel particles detected have sizes from 14 to 60 nm.

The impregnated catalyst shows carbon filaments mostly with diameters around 25 nm, and the detected nickel particles are very homogeneous, around 30–35 nm. The catalyst prepared by thermal decomposition shows carbon filaments with diameters from 18 to 120 nm and nickel particles with large sizes of 160 and 200 nm have been detected.

The XRD diffraction patterns of the spent catalysts show similar results with crystalline phases of metallic nickel and spinels of Ni-Al and Mg-Al. An exception is the diffraction pattern of the catalyst

prepared by thermal decomposition with phases of CeO_2 , spinels of Ni-Al and Mg-Al, NiO and/or MgO and metallic nickel. This result indicates that Ce is either well dispersed or interacts with other phases in all the preparations except for the catalyst prepared by thermal decomposition.

The worst performance displayed by the Ce-containing catalyst prepared by coprecipitation at increasing pH could be due by the big size of the nickel particles detected up to 150 nm, and the carbon filaments with diameters up to 270 nm, both determined from the TEM analysis. The deactivation by carbon deposits is consistent with the observations from previous works both by our group [30,31,36] and by other authors [37]. This catalyst also has the lowest Ni content, as revealed by the ICP-OES analyses. Moreover, the large nickel particles of 150 nm and carbon filaments with diameters of 270 nm observed in the TEM images and by the small peak in the TPR analysis at $268^\circ C$ should be associated. The TPR analysis of the catalyst prepared by coprecipitation at increasing pH shows a small peak at $268^\circ C$ and a low slope at low temperatures which may correspond to NiO having weak interaction with the support. After reduction, unstable large nickel particles are generated in the reaction, as observed by TEM. Christensen et al. [61] showed that the size of the Ni particles significantly influences the resistance of hydrotalcite-derived catalysts against carbon deposition, with smaller Ni crystallites having higher resistance to coke formation.

For the catalyst prepared by coprecipitation at constant pH, scarcely any reduction is observed by TPR at temperatures lower than $435^\circ C$. Thus, the NiO has stronger interaction with the support and after reduction could generate more stable nickel particles than for the catalyst prepared by coprecipitation at increasing pH.

The enhancement of the catalyst stability caused by the incorporation of Ce is evident from the different evolution of the product gas yields over time, as shown in the previous figures. The best results are observed for the catalyst prepared by impregnation. For this catalyst, a low carbon content was determined with very homogeneous small nickel particles and carbon filaments of small diameter. The preparation method of the catalyst provides cerium on the surface, which allows stable nickel particles to be obtained under reaction conditions.

3.2.2. Effect of the Ce content

As described in the previous section, the impregnation method appears to produce the best results at a constant Ce load (3% mass fraction). To test the influence of the cerium content, this preparation method was chosen to produce three different catalysts with 0.5, 1, and 5% (m/m) of this metal, respectively. Table 6 shows the overall results of the gas, liquid and solid yields, as well as the gas composition (on a dry and nitrogen-free basis) of these catalysts. The performance of these materials was compared with the previously prepared catalyst (3%) and with the reference catalyst (previously shown in Table 4).

Fig. 6 depicts H_2 yields from this set of experiments, whereas the evolution of the carbon conversion to gas and the yields to C_2 and CH_4 over time is represented in Fig. 7. Again, the evolution of the yield to CO_2 (not shown) was similar to that of H_2 , and the yield to CO did not show any clear trends. It can be observed that the evolution of the hydrogen yield over time for all the catalysts is somewhat similar, with initial values close to thermodynamic equilibrium and suffering a progressive decay after ca. 20 min of reaction time. Nonetheless, all the Ce-containing catalysts outperform the decay in hydrogen yield of the reference catalyst, except for the 1% Ce catalyst after around 80 min of reaction.

The yields of CH_4 and C_2 s reveal certain trends in their respective evolutions over time. In the case of CH_4 , all the catalysts show a steady increase in the yield to methane with time. There are slight differences between the performances of the different catalysts, showing the following tendency in terms of increased production

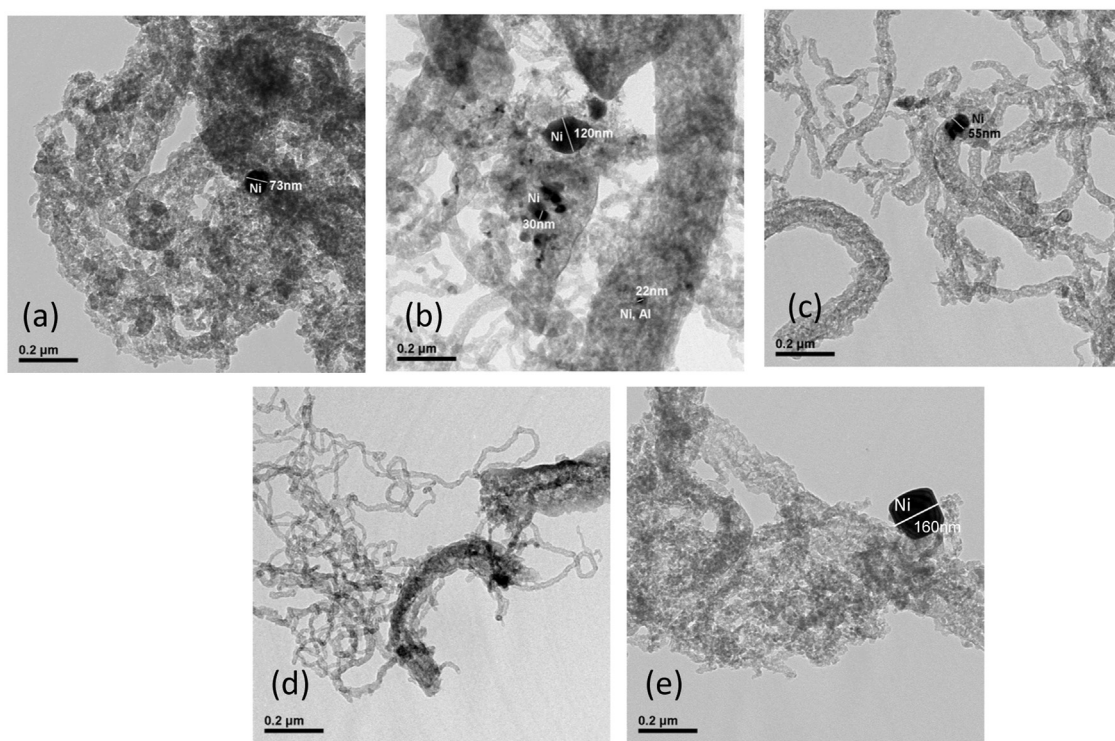


Fig. 5. Representative TEM images of used catalysts with 3% Ce and the reference catalyst (a) Reference, (b) Coprecipitated at increasing pH, (c) Coprecipitated at constant pH, (d) Impregnated and (e) Thermal decomposition.

Table 6

Overall Product yields and gas composition. Experiments with different Ce content. Reaction temperature = 650 °C and $G_{C_1}HSV = 13,000 \text{ h}^{-1}$. Catalysts prepared by impregnation.

	Impregnated, 5% Ce	Impregnated, 3% Ce	Impregnated, 1% Ce	Impregnated, 0.5% Ce
Gas Yield (g/g liquid fed)	0.205	0.193	0.178	0.215
Liquid Yield (g/g liquid fed)	0.729	0.714	0.746	0.707
Solid Yield (g/g liquid fed)	0.016	0.014	0.013	0.015
Average carbon conversion to gas (%)	75.9	72.5	68.1	78.7
Gas composition (vol.%)				
H ₂	69.2	68.8	68.8	70.8
CO	7.1	7.6	8.4	6.8
CO ₂	23.1	22.7	21.7	22.0
CH ₄	0.5	0.6	0.8	0.4

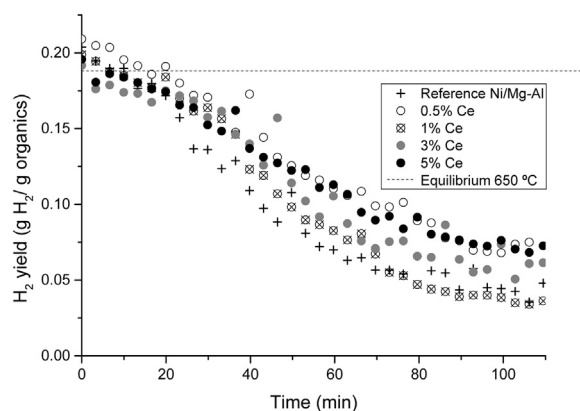


Fig. 6. Evolution of H₂ yield. Experiments with different Ce content. Reaction temperature = 650 °C and $G_{C_1}HSV 13,000 \text{ h}^{-1}$. Catalysts prepared by impregnation.

of methane with time: reference Ni/Al-Mg >1%–3%> 5%> 0.5%. A similar tendency can be found in the yield to C₂s, though the performance of the 1% Ce catalyst is more similar (and after around 60 min

Table 7
Carbon content in spent catalysts prepared by impregnation.

Catalyst	Carbon (%)
Impregnated 0.5%Ce	15.55 ^a
Impregnated 1% Ce	13.63
Impregnated 3% Ce	10.56
Impregnated 5% Ce	10.06

^a Determined by TPO.

slightly worse) to that of the reference catalyst. The increase in the yields to CH₄ and C₂s over time can be related to deactivation by coke deposition on the catalyst surface [31,36]. This fact evidences once again the beneficial effect of adding Ce as a promoter.

Table 7 shows the carbon content in spent catalysts prepared by impregnation. The results indicate a clear tendency of a decrease in the carbon content when the cerium load increases. This can be explained by the oxidative ability of cerium. It can be observed that the decrease in carbon content from 3 to 5% Ce is very small.

Fig. 8 shows representative TEM images of spent catalysts prepared by impregnation with different Ce contents. The impregnated catalyst with 0.5% Ce shows carbon filaments with a wide range of

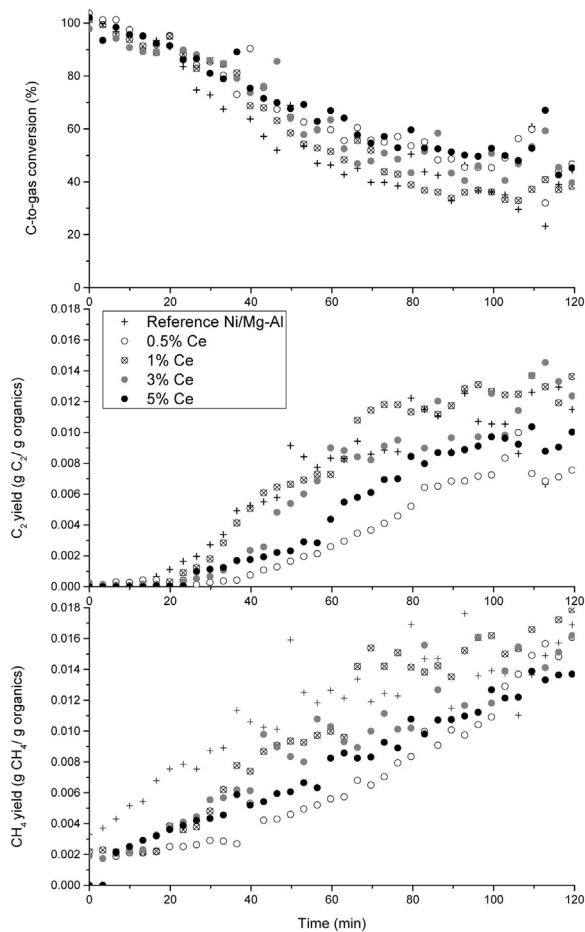


Fig. 7. Evolution of carbon conversion to gas, C_2 and CH_4 yields. Experiments with different Ce content. Reaction temperature = $650^\circ C$ and $G_{C1}HSV = 13,000\text{ h}^{-1}$. Catalysts prepared by impregnation.

diameters from 15 to 108 nm and some nickel particles of 90 nm. The catalyst with 1% Ce shows carbon filaments with roughly two diameter sizes, 24 and around 60 nm. Nickel particles around 20 and 60 nm can be seen. The carbon filaments for the 3% Ce catalyst have diameters around 10 and 25 nm, also homogeneous nickel particles around 30–35 nm. The 5% Ce catalyst shows carbon filaments with diameters around 23 and 82 nm. The nickel particles detected for this catalyst have sizes around 50–70 nm and some around 150–170 nm. The existence of these big nickel particles could be due to segregation of Ni when the Ce load increases. This fact has been cited in the literature [56]. The peak at low temperatures in the TPR profile for the 5% Ce catalyst corroborates the existence of these big nickel particles. These results suggest a relationship between the size of the nickel particles and the diameter of the carbon filaments.

The characterization carried out on the spent catalysts explains the performance of the impregnated 5% Ce catalyst due to the low carbon content. The poor performance of impregnated 1% Ce could be explained by the relatively high carbon content. However, the explanation for the good performance of the impregnated 0.5% Ce catalyst is not clear and requires an in-depth study.

In order to obtain some insights about the good performance of the impregnated 0.5% Ce catalyst, temperature programmed oxidation (TPO) analyses were carried out with the spent samples of the reference catalyst (Ni/Mg-Al) and of the impregnated 0.5% Ce catalyst. Fig. 9 and Table 8 show the results. The quantitative amount of coke has been calculated as g of C/(g of catalyst · g of organics reacted), as already proposed in previous works [32,62]. The g of

Table 8

Carbon quantification results of TPO analyses for Ni/Mg-Al and impregnated 0.5% Ce catalyst used (mg C/(g catalyst · g organics reacted)).

Catalyst	Reference Ni/Mg-Al	Impregnated, 0.5% Ce
Total carbon (mg C/(g cat g org))	170	103
C ($T < 500^\circ C$)	23	18
Temperature main peak ($^\circ C$)	603	613

organics reacted correspond to the organic compounds in the aqueous fraction converted. For this calculation, the carbon conversion to gas was used.

The total carbon for the reference catalyst is 170 mg C/(g catalyst · g organics reacted), this value corresponds to 20.32% of carbon (%) and indicates a good concordance with the value obtained by elemental analysis on Table 5, 20.99%.

The shape of the TPO profiles is very similar (Fig. 9), with the main peak at temperatures of 603 and $613^\circ C$ for the reference and impregnated 0.5% Ce catalysts, respectively. As expected, the total carbon deposited on the spent sample of the reference catalyst is higher than that deposited on the spent impregnated 0.5% Ce catalyst. This tendency is also observed for the carbon deposits that react at temperatures lower than $500^\circ C$. The lower amount of coke on the impregnated 0.5% Ce catalyst than on the Ni/Mg-Al catalyst is in accordance with the results of reforming experiments with the aqueous fraction of bio-oil showing more stability in hydrogen production. In addition, the higher temperature of the main peak of the impregnated catalyst compared to that of the reference catalyst could indicate a higher filamentous nature of the coke, which is also less deactivating.

The total carbon deposited on the impregnated 0.5% Ce catalyst has been compared with that on a NiCo/AlMg catalyst [32] and the results reveal a significant decrease in carbon deposits on the Ce promoted catalyst. The total carbon for NiCo/AlMg catalyst employing the same bio-oil aqueous fraction and fixed bed installation was 129 mg C/(g catalyst g organics reacted). The amount of total carbon deposited on the Ni/Mg-Al catalyst is very similar in these works, indicating the reliability of the comparison. Although the differences caused by the catalyst load are modest, these results suggest that the catalyst containing 0.5% Ce shows a better overall performance under the experimental conditions tested. At the same time, this catalyst contains the minimum amount of Ce, which is beneficial from an economical point of view.

3.2.3. Effect of the aqueous fraction fed

Given the results presented in the previous section, the catalyst containing 0.5% Ce was used for investigating the effect of the different aqueous fractions fed into the system. The main results of these experiments are shown in Table 9.

It can be clearly seen that the two aqueous fractions coming from pine as raw material (RC-Pi and SB-Pi) produce much higher

Table 9

Overall product yields and gas composition. Experiments with different aqueous fraction fed. Reaction temperature = $650^\circ C$, $G_{C1}HSV = 13,000\text{ h}^{-1}$ and 0.5% Ce catalysts prepared by impregnation.

	RC-Pi	SB-Pi	SB-Pp
Gas Yield (g/g liquid fed)	0.215	0.214	0.172
Liquid Yield (g/g liquid fed)	0.707	0.709	0.761
Solid Yield (g/g liquid fed)	0.015	0.017	0.018
Average carbon conversion to gas (%)	78.7	78.1	64.8
Gas composition (vol.%)			
H_2	70.8	68.2	67.2
CO	6.8	8.4	7.5
CO_2	22.0	22.5	24.2
CH_4	0.4	0.7	0.9

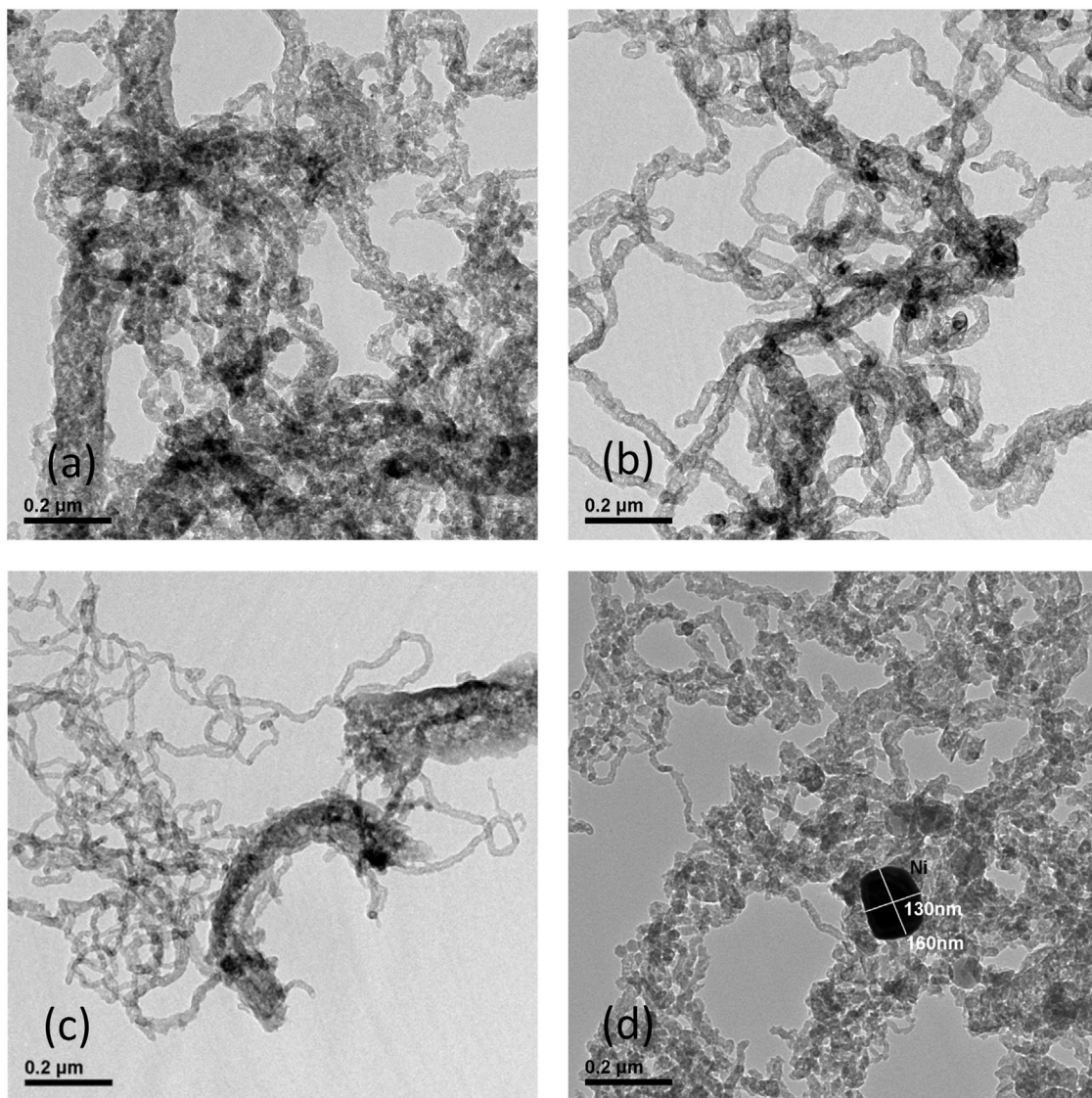


Fig. 8. Representative TEM images of used catalyst prepared by impregnation with different Ce content (a) 0.5% Ce, (b) 1% Ce, (c) 3% Ce and (d) 5% Ce.

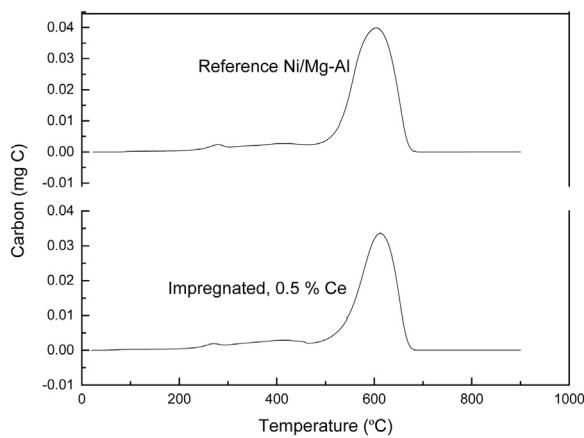


Fig. 9. TPO profiles for spent samples of the Ni/Mg-Al and impregnated 0.5% Ce catalysts.

carbon conversion to gas (of around 78%) and gas yields (0.21) than that coming from poplar (SB-Pp).

Fig. 10 depicts the evolution of H₂ yield with time. The previously mentioned fractions (RC-Pi and SB-Pi) show a distinct

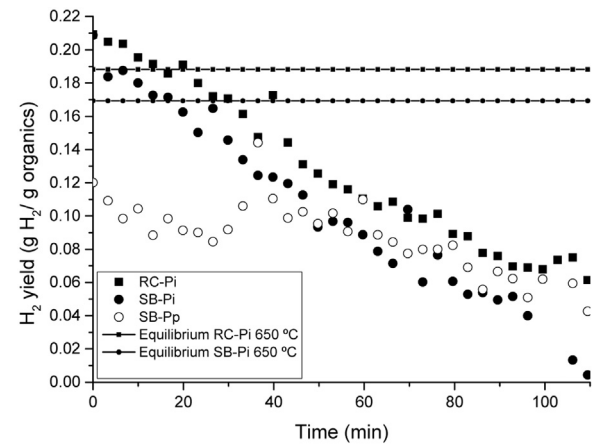


Fig. 10. Evolution of H₂ with time. Experiments with different aqueous fractions. Reaction temperature = 650 °C, G_{C1}HSV = 13,000 h⁻¹ and 0.5% Ce catalysts prepared by impregnation.

behaviour in the first 40 min, with hydrogen production close to the thermodynamic equilibrium declining monotonically, probably

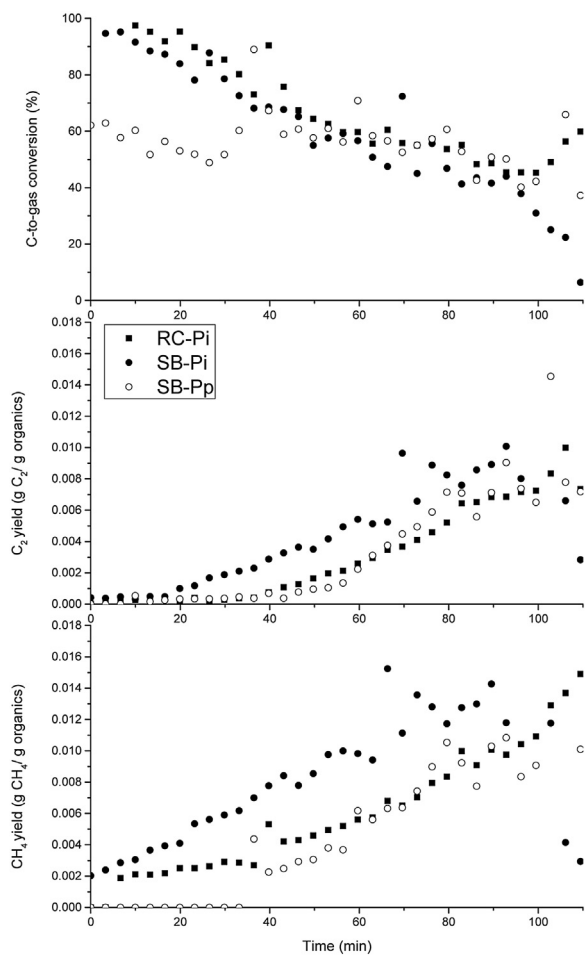


Fig. 11. Evolution of carbon conversion to gas and C₂ and CH₄ yields. Experiments with different aqueous fractions. Reaction temperature = 650 °C, G_{ClHSV} = 13,000 h⁻¹ and 0.5% Ce catalyst prepared by impregnation.

due to catalyst deactivation. SB-Pp show stable values of hydrogen yield in this first stage (and thus, they seem to be unaffected by catalyst deactivation), although significantly far from equilibrium. Because of these differences, RC-Pi and SB-Pi produce their highest H₂ average yields of 0.147 and 0.132 g/g, respectively. Similar trends were found for CO₂ (data not shown).

Thus, the detailed composition of the aqueous fractions (compounds and functional groups) is expected to exert a major influence on hydrogen production, rather than the H/C or O/C ratios. In a previous study of catalytic steam reforming using model compounds, acetol was more easily converted into gaseous products than acetic acid or butanol [21]. Given the role exerted by the Ni-based catalyst, which favours the adsorption of the organics and water and their subsequent reaction [31], it is expected that the interaction of the different organics in the aqueous fraction will depend on their structure and chemical nature. This necessarily affects the catalytic performance and ultimately the product gas composition and yields.

The type of pyrolysis reactor, as well as the main operational conditions such as temperature and residence time, are factors that may influence the aqueous fraction composition, and ultimately the hydrogen yield from catalytic steam reforming.

The trends of the CH₄ and C₂s yields, as shown in Fig. 11, are similar for all the aqueous fractions: gradual increases are found due to deactivation.

The behaviour of the carbon conversion to gas (Fig. 11) is similar to that of the H₂ yield shown in Fig. 10. The aqueous fractions RC-Pi

and SB-Pi show nearly complete conversions at the beginning of the experiment and decline constantly, whereas the SB-Pp values are around 50% for the first 40 min and begin to decline after that time.

The results obtained in this work using the impregnated catalyst with 0.5% Ce content are consistent with the findings of a previous study [63]. The different performance of pine and poplar bio-oil aqueous fractions in catalytic steam reforming is explained by their different chemical composition. The aqueous fraction from poplar generated in a spouted bed has a higher content of acetic acid than the aqueous fraction of pine produced in the same bed [63]. Acetic acid, a significant compound of the aqueous fraction of bio-oil, has been identified as a compound with low reactivity and low coke formation. This explains the lower initial carbon conversion to gas obtained with poplar than with pine aqueous fractions of bio-oil.

4. Conclusions

In this work, Ni/Mg-Al catalysts with varying Ce contents have been prepared using four different methods. The effect of Ce as a modifier has been analysed in the catalytic steam reforming of three different aqueous fractions of bio-oils. The main conclusions are the following:

- (1) The incorporation of Ce to the catalysts has proven to be beneficial in terms of resistance to deactivation of Ni-based catalysts used in the catalytic steam reforming of bio-oil.
- (2) The catalyst preparation method influences the performance of a given catalytic formulation in terms of overall gas yield, yields to different gases and carbon conversion to gas, the best results being obtained with the catalysts in which Ce is incorporated by impregnation. The results are much worse in the case of the catalyst coprecipitated at increasing pH.
- (3) The impregnated catalyst with a Ce content as low as 0.5% (m/m) was found to yield the best results, resulting in a significant decrease in carbon deposits compared to the unpromoted Ni/MgAl reference catalyst and to other previously reported Co- and Cu-modified Ni/MgAl catalysts.
- (4) The initial H₂ yields were similar for the two aqueous fractions derived from pine and higher than the initial H₂ yields produced from poplar. However, the steam reforming of the aqueous fraction from poplar provided a more stable H₂ production.

Acknowledgements

This work was supported by the Spanish MINECO (project ENE2013-41523-R), the Gobierno de Aragón, and the European Social Fund.

The use of the services provided by the Servicio General de Apoyo a la Investigación-SAI, Universidad de Zaragoza, is also acknowledged.

References

- [1] D. Chiaramonti, A. Oasmaa, Y. Solantausta, Power generation using fast pyrolysis liquids from biomass, *Renew. Sustain. Energy Rev.* 11 (2007) 1056–1086.
- [2] A.V. Bridgwater, Biomass fast pyrolysis, *Therm. Sci.* 8 (2004) 21–49.
- [3] C. Briens, J. Piskorz, F. Berruti, Biomass valorization for fuel and chemicals production – a review, *Int. J. Chem. React. Eng.* 6 (2008).
- [4] S. Czernik, A.V. Bridgwater, Overview of applications of biomass fast pyrolysis oil, *Energy Fuels* 18 (2004) 590–598.
- [5] A.V. Bridgwater, Review of fast pyrolysis of biomass and product upgrading, *Biomass Bioenergy* (2011) 1–27.
- [6] M. Samolada, W. Baldauf, I. Vasalos, Production of a bio-gasoline by upgrading biomass flash pyrolysis liquids via hydrogen processing and catalytic cracking, *Fuel* 77 (1998) 1667–1675.

- [7] A.G. Gayubo, B. Valle, A.T. Aguayo, M. Olazar, J. Bilbao, Attenuation of catalyst deactivation by cofeeding methanol for enhancing the valorisation of crude bio-oil, *Energy Fuels* 23 (2009) 4129–4136.
- [8] T. Davidian, N. Guilhaume, C. Daniel, C. Mirodatos, Continuous hydrogen production by sequential catalytic cracking of acetic acid: part I. Investigation of reaction conditions and application to two parallel reactors operated cyclically, *Appl. Catal. A Gen.* 335 (2008) 64–73.
- [9] T. Davidian, N. Guilhaume, H. Provendier, C. Mirodatos, Continuous hydrogen production by sequential catalytic cracking of acetic acid: part II. Mechanistic features and characterisation of catalysts under redox cycling, *Appl. Catal. A Gen.* 337 (2008) 111–120.
- [10] G. Van Rossum, S.R.A. Kersten, W.P.M. Van Swaaij, Catalytic and noncatalytic gasification of pyrolysis oil, *Ind. Eng. Chem. Res.* 46 (2007) 3959–3967.
- [11] D. Wang, S. Czernik, E. Chornet, Production of hydrogen from biomass by catalytic steam reforming of fast pyrolysis oils, *Energy Fuels* 12 (1998) 19–24.
- [12] D. Wang, S. Czernik, D. Montane, M. Mann, E. Chornet, Biomass to hydrogen via fast pyrolysis and catalytic steam reforming of the pyrolysis oil or its fractions, *Ind. Eng. Chem. Res.* 36 (1997) 1507–1518.
- [13] S. Czernik, R. French, C. Feik, E. Chornet, Hydrogen by catalytic steam reforming of liquid byproducts from biomass thermoconversion processes, *Ind. Eng. Chem. Res.* 41 (2002) 4209–4215.
- [14] P.L. Spath, D.C. Dayton, Preliminary screening—technical and economic assessment of synthesis gas to fuels and chemicals with emphasis on the potential for biomass-derived syngas, Tech. Report (2003), NREL/TP-510-34929.
- [15] D. Chen, L. He, Towards an efficient hydrogen production from biomass: a review of processes and materials, *ChemCatChem* 3 (2011) 490–511.
- [16] R. Trane, S. Dahl, M.S. Skjøth-Rasmussen, A.D. Jensen, Catalytic steam reforming of bio-oil, *Int. J. Hydrogen Energy* 37 (2012) 6447–6472.
- [17] F. Bimbela, M. Oliva, J. Ruiz, L. García, J. Arauzo, Hydrogen production by catalytic steam reforming of acetic acid, a model compound of biomass pyrolysis liquids, *J. Anal. Appl. Pyrolysis* 79 (2007) 112–120.
- [18] J.R. Galdámez, L. García, R. Bilbao, Hydrogen production by steam reforming of bio-oil using coprecipitated Ni-Al catalysts, acetic acid as a model compound, *Energy Fuels* 19 (2005) 1133–1142.
- [19] J.A. Medrano, M. Oliva, J. Ruiz, L. García, J. Arauzo, Catalytic steam reforming of acetic acid in a fluidized bed reactor with oxygen addition, *Int. J. Hydrogen Energy* 33 (2008) 4387–4396.
- [20] M.C. Ramos, A.I. Navascués, L. García, R. Bilbao, Hydrogen production by catalytic steam reforming of acetol, a model compound of bio-oil, *Ind. Eng. Chem. Res.* 46 (2007) 2399–2406.
- [21] F. Bimbela, M. Oliva, J. Ruiz, L. García, J. Arauzo, Catalytic steam reforming of model compounds of biomass pyrolysis liquids in fixed bed: acetol and n-butanol, *J. Anal. Appl. Pyrolysis* 85 (2009) 204–213.
- [22] J.A. Medrano, M. Oliva, J. Ruiz, L. García, J. Arauzo, Catalytic steam reforming of model compounds of biomass pyrolysis liquids in fluidized bed reactor with modified Ni/Al catalysts, *J. Anal. Appl. Pyrolysis* 85 (2009) 214–225.
- [23] L. García, R. French, S. Czernik, E. Chornet, *Catal. A Gen.* 201 (2000) 225–239.
- [24] C. Rioche, S. Kulkarni, F.C. Meunier, J.P. Breen, R. Burch, Steam reforming of model compounds and fast pyrolysis bio-oil on supported noble metal catalysts, *Appl. Catal. B Environ.* 61 (2005) 130–139.
- [25] P.N. Kechagiopoulos, S.S. Voutetakis, A.A. Lemonidou, I.A. Vasalos, Hydrogen production via steam reforming of the aqueous phase of bio-oil in a fixed bed reactor, *Energy Fuels* 20 (2006) 2155–2163.
- [26] A.C. Basagiannis, X.E. Verykios, Steam reforming of the aqueous fraction of bio-oil over structured Ru/MgO/Al2O3 catalysts, *Catal. Today* 127 (2007) 256–264.
- [27] S. Czernik, R. Evans, R. French, Hydrogen from biomass-production by steam reforming of biomass pyrolysis oil, *Catal. Today* 129 (2007) 265–268.
- [28] Z. Wang, Y. Pan, T. Dong, X. Zhu, T. Kan, L. Yuan, Production of hydrogen from catalytic steam reforming of bio-oil using C12A7-O⁻ based catalysts, *Appl. Catal. A Gen.* 320 (2007) 24–34.
- [29] G. Van Rossum, S.R.A. Kersten, W.P.M. Van Swaaij, Staged catalytic gasification/steam reforming of pyrolysis oil, *Ind. Eng. Chem. Res.* 48 (2009) 5857–5866.
- [30] J.A. Medrano, M. Oliva, J. Ruiz, L. García, J. Arauzo, Hydrogen from aqueous fraction of biomass pyrolysis liquids by catalytic steam reforming in fluidized bed, *Energy* 36 (2011) 2215–2224.
- [31] F. Bimbela, M. Oliva, J. Ruiz, L. García, J. Arauzo, Hydrogen production via catalytic steam reforming of the aqueous fraction of bio-oil using nickel-based coprecipitated catalysts, *Int. J. Hydrogen Energy* 38 (2013) 14476–14487.
- [32] J. Remón, J. Medrano, F. Bimbela, L. García, J. Arauzo, Ni/Al-Mg-O solids modified with Co or Cu for the catalytic steam reforming of bio-oil, *Appl. Catal. B Environ.* 132–133 (2013) 433–444.
- [33] D. Wang, D. Montane, E. Chornet, Catalytic steam reforming of biomass-derived oxygenates: acetic acid and hydroxyacetaldehyde, *Appl. Catal. A Gen.* 143 (1996) 245–270.
- [34] R.M. Navarro, M.A. Peña, J.L.G. Fierro, Hydrogen production reactions from carbon feedstocks: fossil fuels and biomass, *Chem. Rev.* 107 (2007) 3952–3991.
- [35] M.V. Gil, J. Fermoso, C. Pevida, D. Chen, F. Rubiera, Production of fuel-cell grade H₂ by sorption enhanced steam reforming of acetic acid as a model compound of biomass-derived bio-oil, *Appl. Catal. B Environ.* 184 (2016) 64–76.
- [36] F. Bimbela, D. Chen, J. Ruiz, L. García, J. Arauzo, Ni/Al coprecipitated catalysts modified with magnesium and copper for the catalytic steam reforming of model compounds from biomass pyrolysis liquids, *Appl. Catal. B Environ.* 119–120 (2012) 1–12.
- [37] D. Yao, C. Wu, H. Yang, Q. Hu, M.A. Nahil, H. Chen, et al., Hydrogen production from catalytic reforming of the aqueous fraction of pyrolysis bio-oil with modified Ni-Al catalysts, *Int. J. Hydrogen Energy* 39 (2014) 14642–14652.
- [38] S. Natesakhawat, R. Watson, X. Wang, U. Ozkan, Deactivation characteristics of lanthanide-promoted sol-gel Ni/Al2O3 catalysts in propane steam reforming, *J. Catal.* 234 (2005) 496–508.
- [39] A.C. Basagiannis, X.E. Verykios, Reforming reactions of acetic acid on nickel catalysts over a wide temperature range, *Appl. Catal. A Gen.* 308 (2006) 182–193.
- [40] A.C. Basagiannis, X.E. Verykios, Catalytic steam reforming of acetic acid for hydrogen production, *Int. J. Hydrogen Energy* 32 (2007) 3343–3355.
- [41] T. Davidian, N. Guilhaume, E. Iloju, H. Provendier, C. Mirodatos, Hydrogen production from crude pyrolysis oil by a sequential catalytic process, *Appl. Catal. B Environ.* 73 (2007) 116–127.
- [42] H. Xie, Q. Yu, X. Yao, W. Duan, Z. Zuo, Q. Qin, Hydrogen production via steam reforming of bio-oil model compounds over supported nickel catalysts, *J. Energy Chem.* 24 (2015) 299–308.
- [43] R. Trane-Restrup, S. Dahl, A.D. Jensen, Steam reforming of ethanol: effects of support and additives on Ni-based catalysts, *Int. J. Hydrogen Energy* 38 (2013) 15105–15118.
- [44] K. Bizkarra, V.L. Barrio, A. Yartu, J. Requies, P.L. Arias, J.F. Cambra, Hydrogen production from n-butanol over alumina and modified alumina nickel catalysts, *Int. J. Hydrogen Energy* 40 (2015) 5272–5280.
- [45] P. Fu, W. Yi, Z. Li, X. Bai, A. Zhang, Y. Li, et al., Investigation on hydrogen production by catalytic steam reforming of maize stalk fast pyrolysis bio-oil, *Int. J. Hydrogen Energy* 39 (2014) 13962–13971.
- [46] X. Xu, E. Jiang, Hydrogen from wood vinegar via catalytic reforming over Ni/Ce/y-Al2O3 catalyst, *J. Anal. Appl. Pyrolysis* 107 (2014) 1–8.
- [47] E. Gallegos-Suárez, A. Guerrero-Ruiz, M. Fernández-García, I. Rodríguez-Ramos, A. Kubacka, Efficient and stable Ni-Ce glycerol reforming catalysts: chemical imaging using X-ray electron and scanning transmission microscopy, *Appl. Catal. B Environ.* 165 (2015) 139–148.
- [48] P.N. Kechagiopoulos, S.S. Voutetakis, A.A. Lemonidou, I.A. Vasalos, Hydrogen production via reforming of the aqueous phase of bio-oil over Ni/olivine catalysts in a spouted bed reactor, *Ind. Eng. Chem. Res.* 48 (2009) 1400–1408.
- [49] A. Bhattacharyya, W.D. Chang, M.S. Kleefisch, C.A. Udovic, Catalyst prepared from nickel-containing hydrotalcite-like precursor compound, US Pat. 5767040. <<http://www.google.com/patents/US5767040/>>, 1998 (Accessed 29 July 2016).
- [50] A. Bhattacharyya, Method of hydrocarbon reforming and catalyst precursor, US Pat. 6071433A. <<https://www.google.pl/patents/US6071433/>>, 2000 (Accessed 29 July 2016).
- [51] E. Mikuli, A. Migdal-Mikuli, R. Chyzy, B. Grad, R. Dziembaj, Melting and thermal decomposition of [Ni(H₂O)₆](NO₃)₂, *Thermochim. Acta* 370 (2001) 65–71.
- [52] A. Malecki, R. Gajerski, S. Łabuś, B. Prochowska-Klisch, K.T. Wojciechowski, Mechanism of thermal decomposition of d-metals nitrates hydrates, *J. Therm. Anal. Calorim.* 60 (2000) 17–23.
- [53] R. Martínez, E. Romero, C. Guimon, R. Bilbao, CO₂ reforming of methane over coprecipitated Ni-Al catalysts modified with lanthanum, *Appl. Catal. A Gen.* 274 (2004) 139–149.
- [54] Y. Echegoyen, I. Suelves, M.J. Lázaro, M.L. Sanjuán, R. Moliner, Thermo catalytic decomposition of methane over Ni-Mg and Ni-Cu-Mg catalysts. Effect of catalyst preparation method, *Appl. Catal. A Gen.* 333 (2007) 229–237.
- [55] C.E. Daza, J. Gallego, J.A. Moreno, F. Mondragón, S. Moreno, R. Molina, CO₂ reforming of methane over Ni/Mg/Al/Ce mixed oxides, *Catal. Today* 133–135 (2008) 357–366.
- [56] C.E. Daza, S. Moreno, R. Molina, Co-precipitated Ni–Mg–Al catalysts containing Ce for CO₂ reforming of methane, *Int. J. Hydrogen Energy* 36 (2011) 3886–3894.
- [57] C.E. Daza, J. Gallego, F. Mondragón, S. Moreno, R. Molina, High stability of Ce-promoted Ni/Mg-Al catalysts derived from hydrotalcites in dry reforming of methane, *Fuel* 89 (2010) 592–603.
- [58] O. Lebedeva, D. Tichit, B. Coq, Influence of the compensating anions of Ni/Al and Ni/Mg/Al layered double hydroxides on their activation under oxidising and reducing atmospheres, *Appl. Catal. A Gen.* 183 (1999) 61–71.
- [59] G. Ertl, H. Knözinger, J. Weitkamp, *Handbook of Heterogeneous Catalysis*, 2nd ed., WILEY-VCH, 1997, <http://dx.doi.org/10.1002/9783527610044>.
- [60] I. Suelves, M. Lázaro, R. Moliner, Y. Echegoyen, J. Palacios, Characterization of NiAl and NiCuAl catalysts prepared by different methods for hydrogen production by thermo catalytic decomposition of methane, *Catal. Today* 116 (2006) 271–280.
- [61] K. Christensen, D. Chen, R. Lodeng, A. Holmen, Effect of supports and Ni crystal size on carbon formation and sintering during steam methane reforming, *Appl. Catal. A Gen.* 314 (2006) 9–22.
- [62] L. Di Felice, C. Courson, P.U. Foscolo, A. Kiennemann, Iron and nickel doped alkaline-earth catalysts for biomass gasification with simultaneous tar reformation and CO₂ capture, *Int. J. Hydrogen Energy* 36 (2011) 5296–5310.
- [63] J. Remón, F. Broust, G. Volle, L. García, J. Arauzo, Hydrogen production from pine and poplar bio-oils by catalytic steam reforming. Influence of the bio-oil composition on the process, *Int. J. Hydrogen Energy* 40 (2015) 5593–5608.